ACS Macro Letters

Letter

pubs.acs.org/macroletters

Optimization of the Polymer Coating for Glycosylated Gold Nanoparticle Biosensors to Ensure Stability and Rapid Optical Readouts

Sarah-Jane Richards[†] and Matthew I. Gibson*[,†,‡]

[†]Department of Chemistry and [‡]Warwick Medical School, University of Warwick, Coventry, CV4 7AL, United Kingdom

Supporting Information

ABSTRACT: The development of new analytical tools to probe pathogenic infection processes and as point-of-care biosensors is crucial to combat the spread of infectious diseases or to detect biological warfare agents. Glycosylated gold nanoparticles that change color due to lectin (carbohydrate-binding protein) mediated aggregation may find use as biosensors but require a polymer coating between the particle surface and sugar to ensure stability in complex media. Here, RAFT polymerization is employed to generate glycosylated polymers to coat gold nanoparticles. Rather than being a passive component, it is shown here that the polymer coating has to be precisely tuned to achieve a balance between saline (steric) stability and speed of the readout. If the polymer is too long it can prevent or slow aggregation and hence lead to a poor readout in sensing assays. The optimized glyco-nanoparticles are also demonstrated to be useful for rapid detection of a ricin surrogate.

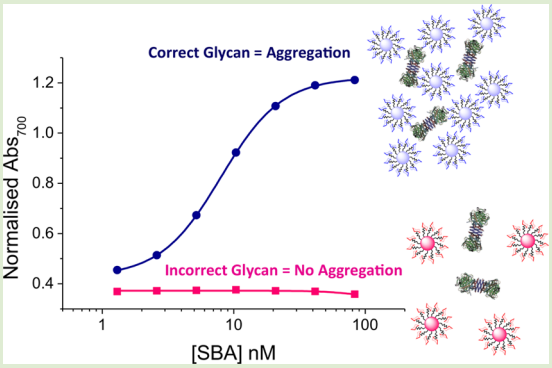

Protein−carbohydrate interactions mediate a multitude of important biological processes, including cell−cell signaling, inflammation, and fertilization;[1,2] however, bacteria, toxins, and viruses also use the carbohydrate moieties on cell surfaces for cell adhesion as the first stage in infection. Lectins are carbohydrate-binding proteins (other than enzymes and antibodies) that interact with carbohydrates noncovalently and reversibly with a high level of specificity.[3,4] The binding affinity of a carbohydrate to its lectin target is typically very weak (10^3−10^6 M^{-1}). This is circumvented in nature by the presentation of multiple copies of the saccharide on the cell surface, this is known as "the cluster-glycoside effect" and, hence, macromolecular structures with a polyvalent presentation of carbohydrates are of interest.[5,6]

Examples of pathogens that exploit the protein−carbohydrate interactions are the FimH adhesin found on the fimbriae of some pathogenic *Escherichia coli* (*E. coli*) that bind to mannose residues on the cell surface of the urinary tract.[7,8] *Vibrio cholerae* secretes a carbohydrate-binding toxin that binds to the GM1 ganglioside on intestinal epithelial cells.[9−11] Ricin is a toxic lectin that presents a potential security threat. It is a lethal, type 2 ribosome-inactivating protein found in the castor bean plant *Ricinus communis*.[12] It is an A-B toxin whereby its B-chain adheres to terminal galactose residues on mammalian cell surfaces, facilitating the delivery of the toxic A-chain into the cytosol of the cell. The A-chain catalyzes the hydrolytic cleavage of a single base from eukaryotic rRNA, leading to a shutdown in protein synthesis and ultimately cell death.[13] The median lethal dose (LD_{50}) of ricin for an adult is estimated to be around 22 $\mu g \cdot kg^{-1}$ of body weight (>1.8 mg for an average adult). Due to its high toxicity and accessibility, its potential as a biowarfare agent has long been recognized, with several recent incidents in the U.K. and the U.S. resulting in threats to public safety; therefore, its rapid detection is highly desirable.

Gold nanoparticles (AuNPs) have been extensively studied as potential biosensors due to their characteristic optical properties and ease of functionalization with a number of biological molecules.[14−24] AuNPs exhibit an intense color in the visible region due to local surface plasmon resonance, which arises due to the collective oscillations of the conduction-band electrons of the gold core.[12,25−27] These optical properties are strongly correlated with their size, shape, dispersion media, and degree of aggregation. Particles larger than 10 nm and smaller than 100 nm exhibit a red coloration; upon aggregation dramatic color change can be observed from red to blue. This is attributed to electric dipole−dipole interactions and coupling between the plasmons of neighboring particles.[16,25] Glyco-gold nanoparticles (glycoAuNPs) are attractive biosensors due to the inherent multivalency of the particles and lectins. The presence of lectins should lead to an optical response as a result of AuNP aggregation, providing the platform for new sensors without the need for expensive equipment and fluorescent- or radio-labeling of proteins. The colorimetric change associated with the aggregation of AuNPs using protein−carbohydrate interactions has been exploited in the detection of lectins[12,28,29] and different strains of influenza.[30] We have shown that

Received: August 10, 2014
Accepted: September 12, 2014
Published: September 16, 2014

dx.doi.org/10.1021/mz5004882 | *ACS Macro Lett.* 2014, 3, 1004−1008

mannosylated glycoAuNPs can be used to distinguish between bacteria with and without Type 1 fimbriae, but that the mode of presentation of the carbohydrates and their distance from the gold surface impacts the detection read-outs, with very slow responses (aggregation) being observed, with polymer coatings limiting their application as point-of-care diagnostics.[31]

Herein we employ RAFT polymerization to generate heterotelechelic polymers that can be conjugated with a glycan at one end and the RAFT-derived thiol at the other to immobilize onto AuNPs. By varying the chain length, the crucial balance between stability in saline media and speed of colorimetric detection is probed for the rapid detection of a series of lectins, including *Ricinus communis* Agglutinin (RCA_{120}), a surrogate for ricin.

Inspired by the glycocalyx on eukaryotic cell surfaces, which has a nonfouling membrane component (phospholipid betaines) with surface immobilized carbohydrates, telechelic polymers were designed with a conjugatable pentafluorophenyl ester at one end and masked thiol (RAFT agent) at the other for gold immobilization, Table 1. The synthetic scheme is shown in Figure 1A. Poly(*N*-hydroxyethylacrylamide) (pHEA) was chosen for its water solubility and non-LCST behavior (unlike PEG methacrylates for example).

Table 1. pHEA Precursor Polymers

[M]/[I][a]	conversion[b] (%)	$M_{n(Theo)}$[c]	$M_{n(SEC)}$[d]	M_w/M_n[d]	DP[e]
10	78	1680	2800	1.14	8
15	87	2250	3500	1.19	13
20	82	2850	4100	1.16	16
25	81	3400	6200	1.10	20
50	80	6300	9400	1.14	40
75	88	9200	12500	1.20	66

[a]Feed ratio of monomer to initiator. [b]Determined by ^{1}H NMR spectroscopy. [c]Theoretical number-average molecular weight, calculated from the feed ratio and percent conversion. [d]Determined by SEC in dimethylformamide (DMF) using poly(methyl methacrylate) standards. M_w = weight-average molecular weight, M_n = number-average molecular weight [e]Theoretical number-average degree of polymerization.

A pentafluorophenol (PFP) trithiocarbonate RAFT agent was chosen to enable facile end-group modification with amino-glycosides[32] and to afford good control with acrylamide monomers.[33,34] The postpolymerization route also means that all the polymers have the same initial chain length distribution and therefore reduce the variability between particle types. Polymers with a degree of polymerization (DP) of 10, 15, 20 25, 50, and 75 were synthesized and their molecular weight distribution was determined by size exclusion chromatography (SEC; Figure 2B), indicating low dispersities (<1.2). The carbohydrates were introduced by a reaction of the PFP end-group with 2-deoxy-2-amino mannose ($ManNH_2$) and 2-deoxy-2-amino galactose ($GalNH_2$). Infrared spectroscopy confirmed the disappearance of the C═O stretch attributable to the carbonyl of the PFP end-group. An advantage of this route is that the glycosylation step also cleaves the trithiocarbonate (RAFT) end group to generate a ω-terminal thiol group. In a subsequent step, the glycosylated, thiol-terminated polymers were incubated with 60 nm AuNPs to enable a monolayer to form. Excess polymer was removed by simple centrifugation-resuspension cycles. 60 nm AuNPs were chosen as the core, as this size range can give lower detection limits in colorimetric assays, as shown previously.[31]

The key aim of this work is to establish the ideal coating parameters to enable *rapid* and *specific* sensing of lectins. We have previously shown[31] that saline stability of gold nanoparticle sensors is crucial to avoid false positives and, therefore, the polymer-coated AuNPS were evaluated by a NaCl titration starting from 1 M, Figure 2A. It was observed that polymers of DP 15 or less were unstable at high salt (>0.2 M, which is close to physiological (0.137 M)) concentrations, making them unsuitable. While longer polymers (predictably) improved saline stability, it is important to consider the effects of having polymers that are too long; these can prevent/slow the rate of aggregation upon addition of the lectins by steric stabilization. The kinetics of particle aggregation (red−blue color change) triggered by the addition of Con A (preferentially binds to α-mannosides) was measured using UV/vis spectroscopy. The change in absorbance at 700 nm (Abs_{700}) was monitored over a period of 1 h for $ManNH_2$-pHEA-AuNPs with polymer linker lengths of DP20, DP50, and DP75. It was found that the shorter linkers resulted in faster aggregation rates (Figure 2B), with the DP75 polymer having no observable changes even after a 1 h incubation. This serves to highlight the delicate balance between stability and sensing for metal nanoparticles, which are modulated by the polymer coating. Guided by these results, a panel of mixtures of DP10/DP20 polymer stabilized particles was synthesized and it was found that a mixture (1:1) of DP10/DP20 polymers affords a coated particle that is saline stable up to 1 M NaCl but retains the ultrafast kinetics of interaction with the partner lectin (blue coloration noted <5 min). Figure 2C shows images of AuNPs with both NaCl and Con A to highlight the optimal formulation and demonstrating that macromolecular engineering is essential to obtain precise and rapid nanobiosensors.

With this optimal polymer coating composition determined, the next stage was to investigate these particles with a series of other lectins to ensure (i) specificity is maintained and (ii) that the coating is universally applicable. In place of $ManNH_2$, $GalNH_2$ was introduced into the polymers to evaluate their binding to SBA (soybean agglutinin) and RCA_{120} (*Ricinus communis* agglutinin). RCA_{120} is particularly important as it is safe to handle relative to the biological warfare agent ricin, and obviously, any new sensory systems for this could find broad applicability. Figure 3A shows the change in UV−vis spectra of $GalNH_2$-pHEA-AuNPs upon addition of 0−85 nM SBA, clearly showing the shift in spectral features from red−blue and an increase in absorbance at 700 nm. The rapid kinetics of the process are shown in Figure 3B, highlighting that ultrafast responses are maintained relative to longer polymer coatings. A video of this color change is included in the Supporting Information for clarity. To ensure specificity, the interaction of SBA with both $GalNH_2$ and $ManNH_2$ particles was evaluated and shown in Figure 3C. The $GalNH_2$ particles show a clear dose-dependent response to the SBA with a low K_d of 8 nM, whereas the $ManNH_2$ particles do not show a K_d in the concentration range tested. Pleasingly, similar results were found for RCA_{120} (Figure 3D), which shows lectin selectivity toward galactose terminal glycans. The $GalNH_2$ functional particles have a K_d of 17 nM, whereas $ManNH_2$ has a far greater K_d of 61 nM, which is to be expected and agrees well with microarray data. Dynamic light scattering was also employed to ensure that aggregation of the particles was the cause of the color change (rather than just surface-binding or precipitation;

dx.doi.org/10.1021/mz5004882 | *ACS Macro Lett.* 2014, 3, 1004−1008

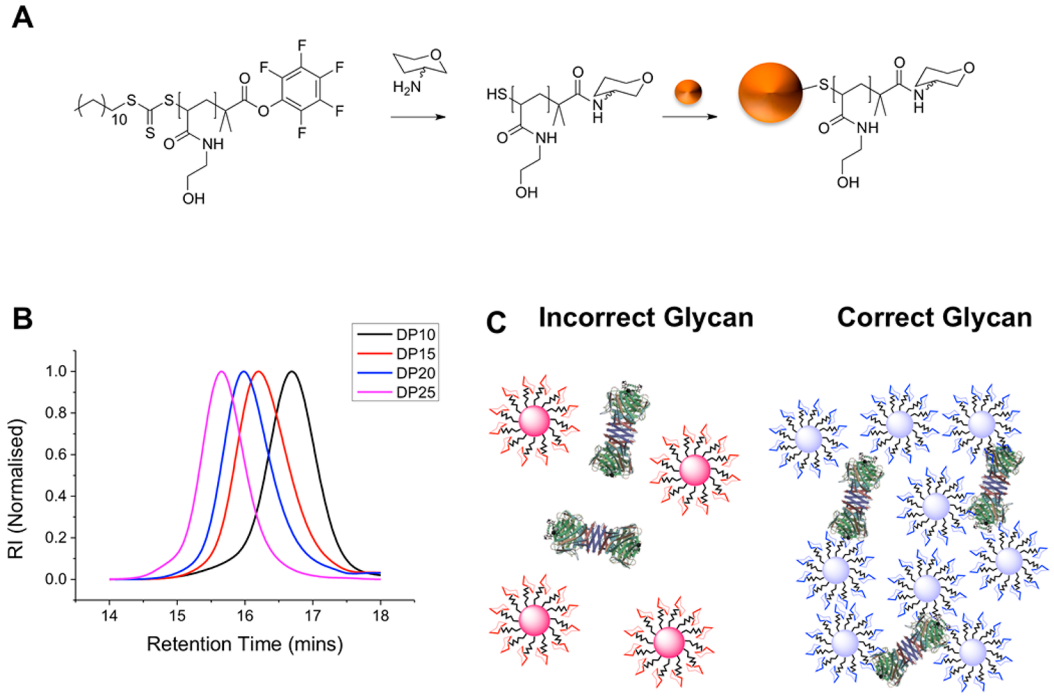

Figure 1. (A) Synthesis of polymer stabilized glycoAuNPs. (B) SEC traces of various molecular weight pHEA polymers. (C) SBA induced aggregation of AuNPs gives rise to color changes with correct lectin glycan pairing.

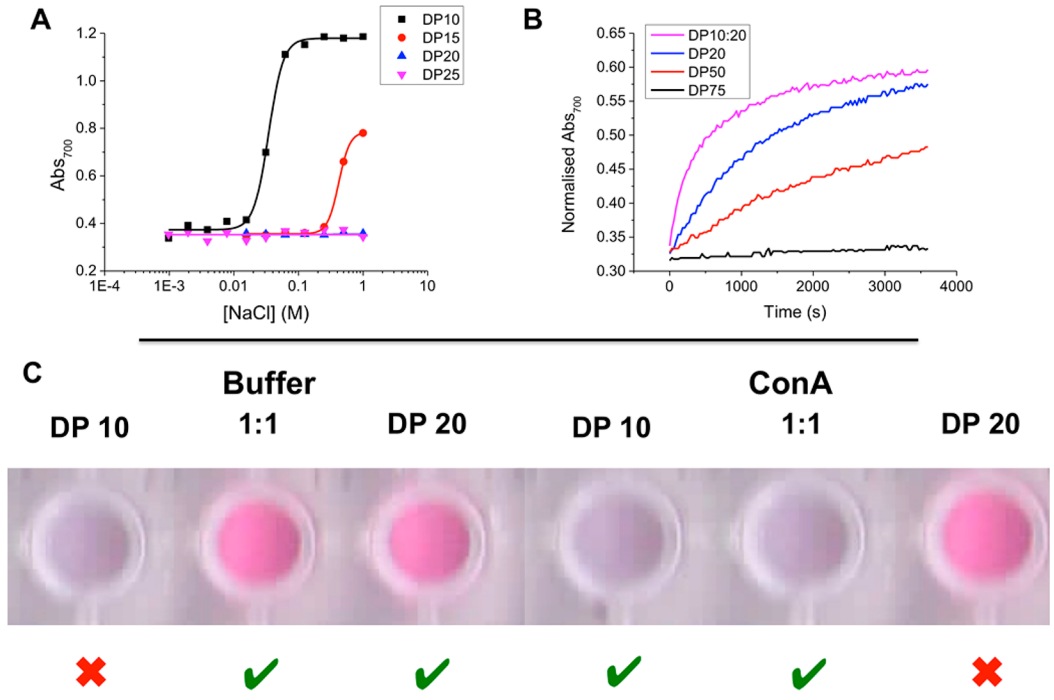

Figure 2. Saline stability and kinetics of Con A induced aggregation. (A) NaCl titration to determine saline stability of polymer coated AuNPs. (B) Kinetics of response of $ManNH_2$-terminated polymer coated AuNP to Con A by UV−vis spectroscopy. (C) Evaluation of the saline stability determined by color remaining red in buffer and speed of color change determined by the color changing from red to blue after 5 min.

Supporting Information). The size changes of the particles were monitored following addition of 85 nM SBA, resulting in the $GalNH_2$ particles rapidly aggregating (as seen by UV−vis), but the $ManNH_2$ particles showed no changes, confirming specificity of this system, which should find broad applicability for large-scale screening of carbohydrate−lectin interactions and point of care biosensors.

In this work, it is shown that coating AuNPs with carbohydrate-functionalized polymers will not always result in a colorimetric assay for lectin binding due to hindrance from the polymer coating. It is crucial to ensure that the polymer is sufficiently long to endow saline stability for use in biological media, but must be balanced against the competing effect that if the polymer is too long, no aggregation events occur (in a reasonable time-scale). Using RAFT polymerization to probe

dx.doi.org/10.1021/mz5004882 | ACS Macro Lett. 2014, 3, 1004−1008

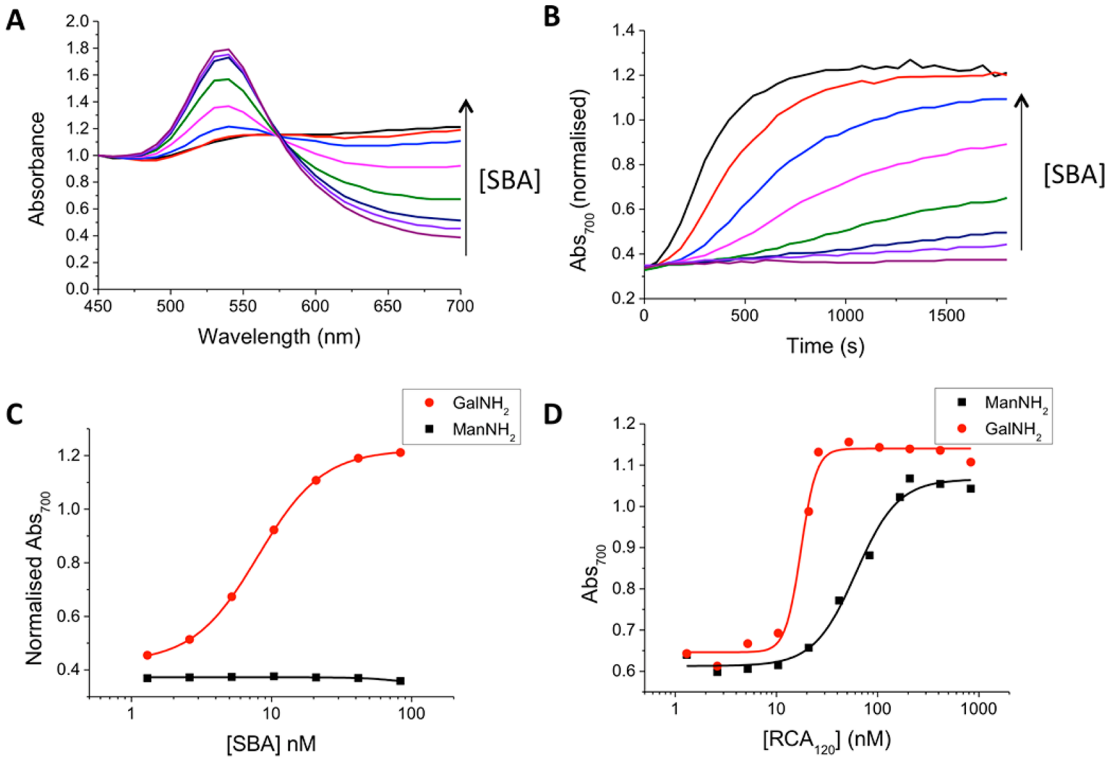

Figure 3. Interaction of $GalNH_2$ and $ManNH_2$ functional AuNPs with SBA. (A) UV−vis spectrum of $GalNH_2$−AuNP upon addition of increasing concentrations of SBA (0−80 nM) following 30 min of incubation. (B) Kinetics of AuNP responses to SBA by monitoring Abs_{700} over 30 min. (C) Binding isotherms (at 37 °C) of $GalNH_2$ and $ManNH_2$ AuNPs with SBA. (D) Binding isotherms (at 37 °C) of $GalNH_2$ and $ManNH_2$ AuNPs with RCA_{120}.

this, it was found that glycosylated poly(*N*-hydroxyethylacylamides) with a DP above 50 were unable to generate a response to lectins, even with the correct sugar in place due to steric stabilization. Through an optimization study, it was found that mixtures of DP10 and DP20 polymers gave rise to stable particles with rapid colorimetric responses. These optimized particles were then employed to study the binding interactions with three different lectins, including a surrogate for ricin, a biological warfare agent, and may be the basis of new point-of-care diagnostics, especially for low-resource environments.

■ ASSOCIATED CONTENT

Supporting Information

Experimental details and video. This material is available free of charge via the Internet at http://pubs.acs.org.

■ AUTHOR INFORMATION

Corresponding Author

*Fax: +44(0)2476 524112. E-mail: m.i.gibson@warwick.ac.uk.

Notes

The authors declare no competing financial interest.

■ ACKNOWLEDGMENTS

Equipment used was supported by the Innovative Uses for Advanced Materials in the Modern World (AM2), with support from Advantage West Midlands (AWM) and part funded by the European Regional Development Fund (ERDF). M.I.G. was a Birmingham Science City Interdisciplinary Research Fellow funded by the Higher Education Funding Council for England (HEFCE). S.J.R. acknowledges the EPSRC MOAC doctoral training center for a studentship.

■ REFERENCES

(1) Bertozzi, C. R.; Kiessling, L. L. *Science* **2001**, *291*, 2357−2364.
(2) Kiessling, L. L.; Gestwicki, J. E.; Strong, L. E. *Angew. Chem., Int. Ed.* **2006**, *45*, 2348−2368.
(3) Ambrosi, M.; Cameron, N. R.; Davis, B. G.; Stolnik, S. *Org. Biomol. Chem.* **2005**, *3*, 1476−1480.
(4) Feinberg, H.; Mitchell, D. A.; Drickamer, K.; Weis, W. I. *Science* **2001**, *294*, 2163−2166.
(5) Lee, Y. C.; Townsend, R. R.; Hardy, M. R.; Lonngren, J.; Arnarp, J.; Haraldsson, M.; Lonn, H. *J. Biol. Chem.* **1983**, *258*, 199−202.
(6) Lundquist, J. J.; Toone, E. J. *Chem. Rev.* **2002**, *102*, 555−578.
(7) Hartmann, M.; Lindhorst, T. K. *Eur. J. Org. Chem.* **2011**, 3583−3609.
(8) Pieters, R. J. *Org. Biomol. Chem.* **2009**, *7*, 2013−2025.
(9) Branson, T. R.; Turnbull, W. B. *Chem. Soc. Rev.* **2013**, *42*, 4613−4622.
(10) Richards, S.-J.; Jones, M. W.; Hunaban, M.; Haddleton, D. M.; Gibson, M. I. *Angew. Chem., Int. Ed.* **2012**, *51*, 7812−7816.
(11) Jones, M. W.; Otten, L.; Richards, S.-J.; Lowery, R.; Phillips, D. J.; Haddleton, D. M.; Gibson, M. I. *Chem. Sci.* **2014**, *5*, 1611−1616.
(12) Schofield, C. L.; Mukhopadhyay, B.; Hardy, S. M.; McDonnell, M. B.; Field, R. A.; Russell, D. A. *Analyst* **2008**, *133*, 626−634.
(13) Fais, M.; Karamanska, R.; Allman, S.; Fairhurst, S. A.; Innocenti, P.; Fairbanks, A. J.; Donohoe, T. J.; Davis, B. G.; Russell, D. A.; Field, R. A. *Chem. Sci.* **2011**, *2*, 1952−1959.
(14) Ghadiali, J. E.; Stevens, M. M. *Adv. Mater.* **2008**, *20*, 4359−4363.
(15) Nusz, G. J.; Marinakos, S. M.; Curry, A. C.; Dahlin, A.; Hook, F.; Wax, A.; Chilkoti, A. *Anal. Chem.* **2008**, *80*, 984−989.
(16) Laromaine, A.; Koh, L. L.; Murugesan, M.; Ulijn, R. V.; Stevens, M. M. *J. Am. Chem. Soc.* **2007**, *129*, 4156−4157.
(17) Singh, A. K.; Senapati, D.; Wang, S. G.; Griffin, J.; Neely, A.; Candice, P.; Naylor, K. M.; Varisli, B.; Kalluri, J. R.; Ray, P. C. *ACS Nano* **2009**, *3*, 1906−1912.

(18) Mayer, K. M.; Lee, S.; Liao, H.; Rostro, B. C.; Fuentes, A.; Scully, P. T.; Nehl, C. L.; Hafner, J. H. *ACS Nano* **2008**, *2*, 687−692.
(19) Huang, S. H. *Sens. Actuators, B* **2007**, *127*, 335−340.
(20) Haes, A. J.; Chang, L.; Klein, W. L.; Van Duyne, R. P. *J. Am. Chem. Soc.* **2005**, *127*, 2264−2271.
(21) Englebienne, P. *Analyst* **1998**, *123*, 1599−1603.
(22) Ohtake, N.; Niikura, K.; Suzuki, T.; Nagakawa, K.; Sawa, H.; Ijiro, K. *Bioconjugate Chem.* **2008**, *19*, 507−515.
(23) Baptista, P. V.; Koziol-Montewka, M.; Paluch-Oles, J.; Doria, G.; Franco, R. *Clin. Chem.* **2006**, *52*, 1433−1434.
(24) Elghanian, R.; Storhoff, J. J.; Mucic, R. C.; Letsinger, R. L.; Mirkin, C. A. *Science* **1997**, *277*, 1078−1081.
(25) Watanabe, S.; Yoshida, K.; Shinkawa, K.; Kumagawa, D.; Seguchi, H. *Colloids Surf., B* **2010**, *81*, 570−577.
(26) Chuang, Y. J.; Zhou, X. C.; Pan, Z. W.; Turchi, C. *Biochem Biophys Res. Commun.* **2009**, *389*, 22−27.
(27) Otten, L.; Richards, S.-J.; Fullam, E.; Besra, G. S.; Gibson, M. I. *J. Mater. Chem. B* **2013**, *1*, 2665−2672.
(28) Lin, C. C.; Yeh, Y. C.; Yang, C. Y.; Chen, G. F.; Chen, Y. C.; Wu, Y. C.; Chen, C. C. *Chem. Commun.* **2003**, 2920−2921.
(29) Jayawardena, H. S. N.; Wang, X.; Yan, M. *Anal. Chem.* **2013**, *85*, 10277−10281.
(30) Marin, M. J.; Rashid, A.; Rejzek, M.; Fairhurst, S. A.; Wharton, S. A.; Martin, S. R.; McCauley, J. W.; Wileman, T.; Field, R. A.; Russell, D. A. *Org. Biomol. Chem.* **2013**, *11*, 7101−7107.
(31) Richards, S.-J.; Fullam, E.; Besra, G. S.; Gibson, M. I. *J. Mater. Chem. B* **2014**, *2*, 1490−1498.
(32) Gibson, M. I.; Froehlich, E.; Klok, H.-A. *J. Polym. Sci., Part A: Polym. Chem.* **2009**, *47*, 4332−4345.
(33) Mayadunne, R. T. A.; Rizzardo, E.; Chiefari, J.; Krstina, J.; Moad, G.; Postma, A.; Thang, S. H. *Macromolecules* **2000**, *33*, 243−245.
(34) Chiefari, J.; Chong, Y. K.; Ercole, F.; Krstina, J.; Jeffery, J.; Le, T. P. T.; Mayadunne, R. T. A.; Meijs, G. F.; Moad, C. L.; Moad, G.; Rizzardo, E.; Thang, S. H. *Macromolecules* **1998**, *31*, 5559−5562.